Adult patients with autoinflammation of unknown origin partially phenocopy the immune presentation of Still's disease.

Rafael Veiga[1,2†], Leana De Vuyst[3†], Julika Neumann[3,4], Leoni Bücken[3], Teresa Prezzemolo[3], Mathijs Willemsen[3,4], Steven Vanderschueren[3,5], Patrick Matthys[3], Immunome Project Consortium for Autoinflammatory Disorders (ImmunAID) ^, Carine Wouters[3,5], Stephanie Humblet-Baron[3*], Adrian Liston[1,2*]

[1] The Babraham Institute, Immunology Programme; Cambridge, United Kingdom.

[2] University of Cambridge, Department of Pathology; Cambridge, United Kingdom.

[3] KU Leuven, Department of Microbiology, Immunology and Transplantation; Leuven, Belgium.

[4] VIB Center for Brain and Disease Research; Leuven, Belgium.

[5] UZ Leuven; Leuven, Belgium.

†,* equal contribution

Correspondence to stephanie.humbletbaron@kuleuven.be or al989@cam.ac.uk

^ ImmunAID consortium : Vassili Soumelis, Arturo Hernandez Cervantes, Thomas Henry, Irina Giurgea, Serge Amselem, Sonia Karabina, Gilles Hayem, Alexandre Belot, Yvan Jamilloux, Eric Hachulla, Thierry Martin, Marie-Elise Truchetet, Nicolas Poursac, Antonine Néel (INSERM), Bruno Fautrel, Stéphane Mitrovic, Emna Chabaane, David Saadoun, Matheus Vieira, Isabelle Koné-Paut, Nasima Matsa, Perrine Dusser, Jean-David Bouaziz, Thibault Mahevas, Sophie Georgin-Lavialle, Keshia Koutekissa, Léa Savey, Pierre Quartier (APHP), Savvas Savvides, Stephanie Humblet-Baron, Adrian Liston, Jeroen Raes (VIB), Carine Wouters, Steven Vanderschueren, Mieke Gouwy, Paul Proost, Patrick Matthys (KU Leuven), Søren Brunak, Isabella Friis Jørgensen, Andres Jimenez Kaufmann, Sara Garcia (UCPH), Philippe Hupé, Fanny Coffin, Apolline Gallois, Henri de Soyres, Julien Roméjon (Institut Curie), Aura Moreno Vega (Owkin), Marc Dubourdeau (Ambiotis), Karoline Krause, Dirk Foell, Christoph Kessel (WWU), Katerina Laskari, Andreakos Evangelos (BRFAA), Paul Van Daele, Clementien Vermont, Rogier van Wijck, Sigrid Swagemakers, Peter van der Spek, Stefan Erkeland, Harmen van de Werken, Yvonne Mueller, Peter Katsikis (Erasmus MC), Michael Hofer, Cem Gabay (Unige), Sinisa Savic, Michael F. McDermott (University Leeds), Helen Lachmann (UCL), Costas Papaloukas, Dimitrios I. Fotiadis (UOI), Dominique de Seny, Christophe Poulet (ULiege), Haner Direskeneli, Seza Ozen, Umut Kalyoncu (Hacettepe), Tadej Avcin (UMCL), Jordi Anton, Violeta Bittermann, Alina Boteanu (HSJD), Marco Francesco Natale, Antonella Insalaco, Emanuele Bizzi, Sonia Caccia, Luca Cantarini, Paolo Sfriso (OPBG), Jean-François Deleuze, Anne Boland (CEA), Sarhan Yaiche (ECRIN).

Abstract:

Autoinflammation of unknown origin remains amongst the most enigmatic of systemic autoinflammatory disorders (SAIDs), immunological disorders characterized by inappropriate activation of the innate immune response. Recent clinical research has identified multiple distinct disorders, although overlap in clinical characteristics and genetic drivers impede rapid and precise diagnosis, and the immunological underpinning of disease is poorly understood. Here we aimed to understand the immunological process behind patients with autoinflammation of unknown origin. In a multi-center European trial, we collected samples from 36 treatment-naïve patients with active disease, and used deep immunophenotyping to compare to 58 healthy controls and an additional demographically-similar 93 SAID patients. Key immunological changes were upregulation of CD38 and HLA across T cell subsets of autoinflammation of unknown origin patients, a trait which partially phenocopied the Still's disease in adult patients. Together this study identifies potential biomarkers and disease-mediators in autoinflammation of unknown origin.

Introduction

Systemic autoinflammatory disorders (SAIDs) are a growing class of immune dysregulation disorders, characterized by inappropriate activation of the innate immune system [1]. Distinct from the better studied set of systemic autoimmune disorders owing to the low level of involvement of the adaptive immune system, it is increasingly recognized that SAIDs are a heterogenous class of disorders, with distinct immunological mechanisms. The recent identification of a genetic basis for many SAIDs has led to a renewed interest in classification and dissection of the underlying pathophysiological causes. In some cases, SAID have a strong genetic background with mutations in single genes. However, they can also be of polygenic or multifactorial origin, with environmental influence modulating the phenotype [2]. To date, this process has identified more than 56 Mendelian drivers of SAID, and more than 40 different clinical presentations, with overlapping phenotypic features, genetic associations and immunological drivers associated with the diverse SAIDs [3, 4, 5].

Several SAIDs have a long-standing recognition as distinct pathologies. In 1930, a first case of what we now recognise as Familial Mediterranean Fever (FMF) was reported [6], a periodic fever syndrome which is one of the most common monogenic SAIDs. By 1997, mutations in the *MEFV* gene, which encodes the protein pyrin and upon activation forms an inflammasome, were identified as the driving force behind FMF [7, 8]. Since the 1970s, FMF has typically been treated with colchicine [9, 10]. Other SAIDs, however, were long neglected as research subjects, in part due to the rarity of these conditions in individual medical centres. Recent investments in clinical research into SAIDs, with modern research techniques and multi-center consortiums of geneticists, clinicians and scientists in the field, have led to remarkably rapid progress in both understanding the underlying biology and in rational selection of pharmacological interventions. For example, Masters *et al.* identified a new variant in the *MEFV* gene that leads to Pyrin-Associated Autoinflammation with Neutrophilic Dermatosis (PAAND), a distinct disease from FMF with partially overlapping but unique clinical presentations [11]. The distinctive excessive IL-1β production in PAAND suggested disease control using IL-1β antagonists, demonstrating the value of mechanistic understanding in rational drug selection. Other SAIDs have also seen large advances in understanding the genetic basis, such as Behçet's disease (BD). In Behçet's, with vascular and tissue inflammation, association with the HLA-B*51 gene has been long established, although it accounts for only 20% of the genetic risk [12, 13]. More recently, Remmers et al. identified additional associations with the *IL10* and *IL23R-IL12RB2* loci using a genome-

wide association study (GWAS) approach [14]. Numerous studies have found associations between various cytokines and BD, influencing both disease onset and severity [15]. Nevertheless, the cellular landscape of BD, and most other SAIDs, remains enigmatic, leaving the full understanding of its pathophysiology incomplete.

Within the spectrum of SAIDs, *undifferentiated autoinflammatory diseases* (also referred to as *undefined SAIDs* and as *syndrome of undifferentiated recurrent fevers (SURF*)) represent a particularly enigmatic group of conditions [16]. These patients have systemic inflammation with increased CRP levels and symptoms of an autoinflammatory disease (fevers, fatigue, rash, arthralgia), in the absence of a molecular diagnosis and without fulfilling the clinical criteria of a distinct polygenic or multifactorial SAID [2, 17]. In the current study, we use the term *autoinflammation of unknown origin* to designate patients who present with recurrent fevers and increased acute phase reactants (CRP >30mg/L or SAA > 25 mg/L) occurring over more than 3 months. At present, it is not entirely clear whether autoinflammation of unknown origin represents an individual disease entity or refers to an amalgamation of multiple different conditions. It also may comprise a diverse group of patients with atypical presentations of a defined SAID. This complexity presents significant challenges to patient care, complicating both treatment strategies and accurate prognosis, acknowledging that in broader cohorts of patients with autoinflammation of unknown origin, up to 30% to 50% of the patients remains with no definitive diagnosis [18, 19].

Progression on understanding the pathophysiology of inflammation of an unknown origin will rely on multi-center studies and the application of systematic immunological analysis. Here we report on a collaboration across 30 European medical centers, which collected samples from 36 patients with active disease, diagnosed as having autoinflammation of unknown origin and naïve of immunomodulating agents. Critically, we were able to compare these patients not only to 58 healthy controls, but to an additional 93 treatment-naïve SAID patients and with active disease sharing key demographic features, allowing a direct comparison of the immunological state across these conditions. High parameter flow cytometry analysis identified autoinflammation of an unknown origin as a relatively distinct immunological state, with the greatest similarity to Still's disease in adult patients. These data suggest that autoinflammation of unknown origin is a relatively discrete disease entity at the cellular immune level, and highlight the potential benefit of investigating shared genetic causes and treatment responses to AOSD patients.

Results

Identification of immune phenotypes in autoinflammation of an unknown origin

To develop an insight into the immunological events associated with autoinflammation of an unknown origin, a large number of patients with a spectrum of active systemic autoinflammatory disease across 30 participating European hospitals were recruited. Patients were enrolled with active disease and naïve of immunomodulating agents, with peripheral blood mononuclear cells (PBMCs) collected, and patients diagnosed according to the respective SAID diagnostic criteria (**Table 1**). Our study included 36 patients classified as having autoinflammation of unknown origin, and an additional 93 patients with well-defined SAIDs following a molecular diagnosis or internationally approved clinical criteria. The selection of SAIDs was based on availability of sufficient samples for statistical comparison and on a similar demographic profile compared to the group autoinflammation of unknown origin. This resulted in 35 patients with Still's disease (a polygenic/multifactorial SAID characterised by persistent high fevers, rash and joint symptoms), 35 patients with FMF (a prototypic monogenic hereditary fever syndrome) and 23 patients with Behçet's disease (a polygenic/multifactorial SAID characterised predominantly by aphthosis, ocular symptoms and vasculitis). Patients diagnosed in rare disease categories, or disease categories with significantly different demographic profile, were excluded from the analysis, due to insufficient power to run statistical analysis. An additional 58 healthy individuals, recruited simultaneously, were included, for a total of 187 individuals. Each set of PBMCs was analysed by high parameter flow cytometry and gated for 208 defined immunological subsets, covering the major leukocyte populations present in PBMCs. This dataset, available as a resource, was used to assess the immune phenotype of patients presenting with autoinflammation of an unknown origin and other well-defined systemic autoinflammatory diseases without the confounding effects of treatment.

Before performing a multi-disease analysis, we first compared the immune status of patients with autoinflammation of unknown origin to healthy individuals. Using a multivariate logistic regression, adjusted for sex and age, we identified the immune parameters significantly associated with autoinflammation of unknown origin (**Figure 1A, Supplementary Figure 1**). The first 40 parameters added the greatest explanatory power to discriminate between autoinflammation of unknown origin and healthy individuals (**Figure 1B**). Of these, the strongest effects were increases in CD38+ subsets (including within the CD27- CD8+ T cell subset, within

the total CD8+ T cell population, within the NKT cell population, within CD16+ NK cells, within DN T cells, and within NK cells), decreased IgM+ IgD+ memory B cells, decreased BAFF-R^{high} naïve B cells (among IgM+IgD+ naïve B cells and IgM^{low} IgD+ naïve B cells) and decreased HLA-DR+ cells within the CD16-CD56^{dim} NK population (**Figure 1C**). The aggregate of data in the 40 highly associated parameters was highly discriminatory against healthy individuals, with an AUC of 0.86 (**Figure 1D**). While the full set of immune parameters poorly separated autoinflammation of unknown origin patients from healthy individuals (**Figure 1E**), indicative of non-disease variation being the primary driver of diversity in the dataset, the top 10 parameters (from figure 1A) discretely separated the populations (**Figure 1F**). Notably, while these immunological changes were highly discriminatory between the autoinflammation of unknown origin patients and the healthy individuals, the strongest parameters had poor discrimination with other systemic inflammation patient sets in our data set, with the Still's disease population in particular showing similar or greater changes in each parameter (**Figure 1C**). Together, these data suggest that autoinflammation of unknown origin is a discrete immunological condition, or a collection of different conditions with a similar immune signature with patients clustered together on the basis of consistent changes compared to healthy individuals.

Immunological changes across systemic autoinflammatory diseases

The identification of an immunological profile shared across autoinflammation of unknown origin patients suggests a common underlying immunological process. We next sought to determine whether this immunological profile was shared with other systemic inflammatory diseases, or constituted a unique immunological entity. Based on the referred to systemic autoinflammatory diseases, with similar demographic profiles, in the participating hospitals, we had patient datasets available with Still's disease, FMF and Behçet's disease.

We first performed a disease vs healthy multivariate logistic regression for each disease in isolation. Still's disease presented with a strong immunological phenotype (**Figure 2, Supplementary Figure 2**), with the greatest change observed in parameters associated with elevated CD38 expression (in CD8+ T cells, DN T cells, NKT cells, CD16+ NK cells and CD27-CD4+ T cells) and a higher fraction of HLA-DR+ cells (within CD4+ T cells, and CD4+ T cell subsets). Strong separation between disease and healthy immunophenotype was observed even when all immunological parameters were used (**Figure 2E**) and was enhanced when the top 10 parameters were used (**Figure 2F**). While these parameters were selected in a healthy-Still's disease comparison, the major immunological changes also separated Still's disease from

the other disease states (**Figure 2C**). FMF, by contrast, presented with weaker immunological differences from the healthy population (**Figure 3, Supplementary Figure 3**). Key immunological changes included decreased NK cell number (yet with increased frequency of the CD11c+ NK subset), increased frequency of CD40+ cells within B cell subsets, and changes to CD38 and HLA-DR expression similar to Still's disease but far weaker in magnitude (**Figure 3C**). Behçet's disease presented with a similar pattern to FMF (**Figure 4, Supplementary Figure 4**). Differences between Behçet's and healthy individuals were generally low in magnitude, with the key changes being a drop in NK cells (accompanied by increased CD94+ expression in NK cells), changes to the monocyte population (decreased non-classical monocytes and HLA-DR+ monocytes), and increased non-switched memory B cells (**Figure 4C**). Together, these separate analyses broadly suggested divergent programs in the systemic inflammatory diseases analysed, with autoinflammation of unknown origin associated with similar parameters to Still's disease, while FMF and Behçet's had distinct, and weaker, immunological changes.

Autoinflammation of unknown origin partially phenocopies Still's disease

To formally compare between diseases, we turned to a multi-disease machine learning approach. To identify the discriminators between diseases, we built a Random Forest algorithm without healthy individuals in the training set, while including healthy individuals in the analysis post-parameter selection. The model identified a complex set of immunological parameters which, when used together, provided discriminatory capacity between diseases (**Supplementary Figure 5**). The developed model was tested for discriminatory capacity via Receiver Operating Characteristic (ROC) curves in pair-wise comparisons (**Figure 5**). The model varied in its discrimination power depending on the disease comparisons made. For autoinflammation of unknown origin, discrimination power was highest against healthy individuals (0.94), lowest for Still's disease (0.79) and FMF (0.80) and intermediate for Behçet's (0.85). Still's disease had strong discrimination power between all conditions, except autoinflammation of unknown origin, while FMF and Behçet's showed relatively weak discrimination, except in comparison to Still's disease (**Figure 5**). Using an independent approach, with a PCA-based comparison, again built only on the four disease groups, individuals formed two main clusters – one including healthy, FMF and Behçet's individuals, and one including Still's disease and autoinflammation of unknown origin individuals (**Figure 5**). Together, these data demonstrate that immune phenotype is effective in discriminating autoinflammation of unknown origin and Still's disease from healthy individuals and patients with

FMF and Behçet's, while disease-specific signatures were weaker components of the variation observed.

The immunophenocopying of Still's disease in autoinflammation of unknown origin patients was also observed when looking at the key explanatory immune parameters in isolation (**Figure 6**). For multiple parameters, changes between Still's disease and autoinflammation of unknown origin moved in tandem, while individuals in the other diseases remained unchanged. BAFF-R expression (in the total B cell population and multiple subsets of naïve and transitional B cells) behaved in this manner. For other parameters, chiefly CD38 expression (in CD27- CD8+ T cells and DN T cells) and HLA-DR expression (across multiple T cell subsets), the phenotype was strongest in Still's disease, with autoinflammation of unknown origin moving in a similar direction but to a lower extent (especially with HLA-DR upregulation). The only exception among the major parameters was CD11c+ CD16+ NK cells, which were enriched in both Still's disease and FMF, and normal in the other diseases. Together, these individual immunological changes, among the most inter-disease discriminatory in nature, support the conclusion that autoinflammation of unknown origin partially phenocopies the cellular immunological presentation of Still's disease, while being a distinct immunological entity to the other systemic inflammatory conditions tested.

Discussion

The number and scope of SAIDs continue to grow thanks to increased clinical recognition and collaborations worldwide, as well as continuous advances in molecular diagnosis. As SAIDs are a heterogeneous family of rare disorders with significant overlap in clinical characteristics, nonspecific symptoms and multi system involvement, a rapid and precise diagnosis is often challenging. For instance, recent publications have highlighted the continuum between Still's disease and other systemic inflammatory disorders and distinguishing Still's disease from other SAIDs can be challenging considering monogenic autoinflammatory conditions, Schnitzler syndrome or Sweet syndrome in addition to sarcoidosis or spondylarthritis[20, 21]. Similarly, Behçet's disease shares features with inflammatory bowel disease and other types of vasculitis, complicating its diagnosis [22]. As a result, long-term follow-up is often required to identify diagnostic distinctness, especially in systemic conditions.

Understanding the genetic and immunological drivers of these disease could aid in diagnosis. Surprisingly, unlike autoimmune diseases, which are generally multigenic, many SAIDS follow Mendelian inheritance patterns, providing the potential for gene-informed clinical diagnosis. Despite the attractiveness of genetics as a simple diagnostic, in practice even the Mendelian disorders show complex genotype-phenotype relationships, with single clinical entities having multiple different genetic causes and mutations in the same genes being the drivers in multiple different disorders [23]. This genetic pleiotropy and heterogeneity complicate accurate diagnosis and there is thus a need for other biomarkers to aid diagnosis. As a functional driver of clinical presentation, immunological changes are among the most attractive potential biomarkers for SAIDs. This is especially in cases of autoinflammation of unknown origin, where the diagnosis is currently based on the slow exclusion of other SAIDs, along with the use of classification criteria and FDG-PET scans. While the involvement of certain immune players is known for some SAIDs [24], the detailed immunophenotyping of other patient sets remains incomplete, and the degree to which immunological changes will be able to aid diagnosis remains undetermined.

This study aimed to facilitate the diagnostic process of one of the most enigmatic SAIDs, undifferentiated autoinflammatory diseases (autoinflammation of unknown origin in this manuscript), by defining the specific immune phenotype. To thoroughly study the immune signature of autoinflammation of unknown origin, large cohorts of treatment-naïve patients are necessary, since defining immunological drivers is further complicated by the treatments patients receive. In addition to testing patients naïve of treatment, it is important to include relevant controls, rather than only heathy individuals. Pan-inflammation markers such as CRP are diagnostically useful in identifying patients with inflammation, but have poor discriminatory power to provide finer level diagnosis. The comparative groups used here were SAID patients naïve of treatment with similar demographic characteristics, allowing a cross-condition comparison.

By comparing patients with different SAIDs (including autoinflammation of unknown origin, Still's disease, Behçet's disease and FMF) to each other and to healthy individuals, valuable information could be identified distinguishing disease states. Multiple immunological signatures were identified across the diseases, with the key discovery being the partial immunophenocopying observed between autoinflammation of unknown origin and Still's disease. Previous studies have demonstrated altered B cell subsets in Still's disease patients, compared to healthy individuals [24, 25]. Our data, however, additionally suggest an important role for T cells, as supported by Myachikova et al [26]. T cells in the synovial fluid have already been

shown to play an important role in the disease phenotype of juvenile idiopathic arthritis [27], and CD4+ and CD8+ T cells locally play an important role in tissue-specific inflammation and disease relapse [28]. Our findings specifically showed that CD38 and HLA-DR expression in multiple T cell subsets was associated with Still's disease. Jung et al. have also reported elevated HLA-DR expression in Still's disease patients, though they also noted decreased CD4+ and CD8+ cells [29]. Interestingly, a similar phenotype to our observation, expansion of CD38+ HLA-DR+ cells within CD4+ T cells, CD8+ T cells and NK cell populations, has been associated with macrophage activation syndrome, a life-threatening complication of Still's disease, and to a lesser extent in patients with systemic juvenile idiopathic arthritis [30]. This elevated CD38 and HLA-DR expression in patients with autoinflammation of unknown origin, although to a lower extent than that observed in Still's disease patients, underscores the need to further explore the role of T cells and their activation as a potential clinical driver in autoinflammation of unknown origin despite the common assumption that autoinflammation is predominantly associated with innate immunity dysregulation. An additional intriguing finding from our study is the overlap in immune signatures between FMF and Behcet's disease, where the discrimination between these two conditions were the most challenging. Notably, clinical and genetic overlap has also been observed in both diseases with pathological variants of *MEFV* identified in both diseases, further reinforcing the potential connection between them [31].

There are several key limitations to this study. Although multi-center, the study needs to be independently verified, to determine if the changes observed are reproducible across multiple cohorts. The phenotypes observed here in these treatment-naïve patients likely reflect different stages of disease as they were at varying points in their disease onset; there is potential for an immunological evolution during disease progression. Diagnostic criteria for SAIDs are notoriously difficult to implement, and some patients defy simple categorization, impeding simple replication studies. Finally, PBMC sample preparation and flow cytometry analysis is more technically variable than serum-based biomarker analysis, and the phenotypes observed here may be sensitive to changes in processing or analysis. However, even noting these limitations, the parallels between autoinflammation of unknown origin and Still's disease provide actionable research pathways. The phenotypes observed here could be incorporated into biomarker studies to aid in diagnostics. Genetic similarity could also be tested, using known Still's disease genetic drivers as candidate genes in autoinflammation of unknown origin. Finally, immunophenocopying could potentially be accompanied by parallel treatment response. Still's disease is typically treated with corticosteroids, methotrexate, IL1 blockade and anti-IL6

biotherapies. The study here, following replication, might provide a rationale for testing effective Still's disease regimes in patients with severe autoinflammation of an unknown origin as no specific drug is currently recommended and early treatment is essential for preventing complications such as amyloidosis and further organ damages. The beneficial response to IL1 blockade of the majority of tested patients with undifferentiated systemic autoinflammatory disorder [32, 33, 34], as observed in Still's disease, provides further support for exploring this approach.

Methods

Study design and patient's characteristics

The study was designed to investigate immune signatures and to define biomarkers specific to different autoinflammatory disorders, in order to allow better disease stratification and faster as well as more precise diagnosis. This study was conducted within the Immunome project consortium for AutoInflammatory Disorders (ImmunAID). 450 patients with different systemic autoinflammatory disorders (SAID) and healthy controls were enrolled from 30 clinical centers throughout Europe and Turkey, to assure a broad inclusion of SAID subtypes and a sufficient number of individuals for rare diseases. For Still's disease, Behçet's disease and Familial Mediterranean Fever (FMF), existing and validated international classification criteria were used. For autoinflammation of an unknown origin, without existing classification criteria, patients were selected with idiopathic and recurrent systemic inflammation according these following criteria; Temperature >38°C during flare, CRP> 30mg/L or SAA>25mg/L on at least 3 occasions separated by 2 weeks and symptom occurring over a period of more than 3 months. Active disease was defined with presence of fever, CRP> 30mg/L and Physician Global Assessment (PhGA) >2/10. Exclusion criteria included infection, antibiotic treatment in the last 2 weeks, autoimmune diseases, evidence of immunodeficiency or neoplasia. Healthy individuals (free of inflammatory disorders) were used as a control group regarding baseline immune parameters. Demographics of the healthy and patient populations are given in **Table 1**. All individuals were naïve of treatment from anti-inflammatories and individuals with active treatment were excluded from further analysis. From the ImmunAID cohort, 52 patients were diagnosed with Still's disease in adults, 34 with Behçet disease, 49 with FMF, 71 with autoinflammation of unknown origin and additional 72 healthy controls were included. After exclusion of patients receiving treatment, patients without available samples, and patients with sample of poor quality to perform further analysis, we enrolled in our study 35 patients diagnosed with Still's disease in

adults, 23 with Behçet disease, 35 with FMF, 36 with autoinflammation of unknown origin and 58 healthy controls.

All individuals provided written informed consent for data collection, sampling and analyses. Sample collection was performed according to the local ethical requirements. Participants had blood drawn to collect peripheral blood mononuclear cells on site. Samples were frozen and locally stored in liquid nitrogen. Samples were shipped to a central laboratory in batches, and stored in liquid nitrogen until further analysis.

PBMC isolation and flow cytometry

PBMCs were isolated from EDTA whole blood by density gradient centrifugation, using LSM (lymphocyte separation medium, MP Biomedicals) according to the manufacturer's recommendations, frozen in Cryostor CS10 (Stemcell technologies) and stored in liquid nitrogen. Frozen PBMCs were thawed in complete RPMI, washed twice, and stained with live/dead marker (fixable viability dye eFluor780) in the presence of an Fc receptor binding inhibitor cocktail (both eBioscience). Additionally, cells were stained with the following fluorochrome-conjugated antibodies: anti-CD3 (REA613, Miltenyi Biotec), anti-CD123 (7G3), anti-CD80 (L307.4), anti-CD21 (B-ly4), anti-CD27 (L128), anti-BAFF-R (11C1), anti-CD94 (HP-3D9), anti-CD86 (2331 (FUN-1)), anti-CD141 (1A4), anti-CD56 (NCAM16.2), anti-CD4 (SK3), anti-CD16 (3G8), anti-CD40 (5C3, all BD Biosciences), anti-CD8 (RPA-T8), anti-CD57 (HNK-1), anti-CD24 (ML5), anti-HLA-DR (L243), anti-CD19 (HIB19), anti-IgM (MHM-88), anti-CD11c (3.9), anti-IgD (IA6-2), anti-CD10 (HI10a), anti-CD38 (HB-7, all BioLegend), anti-CD14 (TuK4, eBioscience). Cells were then fixed using the Foxp3/Transcription factor buffer staining set (eBioscience) and data were collected on a BD FACSymphony A3 Cell Analyzer (BD Biosciences). Data from .fcs files were compensated with AutoSpill [83] and manually pre-processed in FlowJo to exclude non-cellular events. Gating was performed in R (version 4.0.2) with a custom script (Neumann *et al*., manuscript in preparation), automatically calculating subset boundaries between populations listed in **Supplementary Spreadsheet 1**.

Systems immunology analysis

The custom script for automatic gating was set to identify 261 different cell populations or subpopulations with distinct phenotypes. Following the automated gating, a manual curation of the data was conducted, which found variation in CD80 marker detection resulted in low

identification capacity, resulting in exclusion from the analysis. Variation in low-frequency subsets made the calculation of sub-populations from these subsets difficult, due to missing data. To maintain comparability between individuals and consistency within the database, we excluded cell populations with more than 20% missing data. Consequently, data analysis was performed on a set of 208 immune variables (cell population frequencies).

Data Imputation

To address missing data, data was imputed, resulting in a reduction in data precision rather than data loss. K-nearest neighbors (KNN) imputation [35] was used to maintain data heterogeneity and provide good accuracy. Unlike imputation methods based on central tendency and regression models, KNN imputation does not significantly reduce data heterogeneity. Each cellular variant frequency exhibited its own unique distribution and magnitude. To prevent highly skewed distributions and large values from disproportionately influencing the distance measures, a Box-Cox transformation [36] was applied, followed by standardization prior to imputation. This process normalized the data, ensuring that the resulting dataset contained information more comparable in their metrics, for a more robust and consistent database for subsequent analyses.

Identification of cell frequencies associated with disease

For independent analysis of cell frequency association, we employed multivariate logistic regression for each cellular variant, using sex and age as confounding variables. The outcome variable in these regressions was the presence of each pathology compared to healthy controls, allowing the isolation of the specific contribution of each cellular subset to the disease state.

To select the most associated markers, first all markers with a p-value less than or equal to 0.05 were identified. Among these significant markers, markers were ranked based on the magnitude of the effect, using the odds ratio (OR) as the criterion. The optimal number of markers to include in the model was assessed using multivariate logistic regression with L2 penalization (ridge regression). This penalization reduces numerical instability and limits potential overfitting. The model was run with 1 to 200 variants together, in order of importance. For each of these 200 models, executed randomly 200 times using 5-fold cross-validation, outcome was stratified to capture the lower number of immunological variables with highest explainability and generalization.

The optimal number of markers necessary to explain each disease was identified by analyzing the behavior of the average area under the ROC curve (AUC) across the validation groups for each number of variants.

Describing similarities between different pathologies

To visualize the similarities between different pathologies in relation to the control group, principal component analysis (PCA) focusing on the first two principal components was used. PCA analysis was run both on all cell frequencies in the dataset, where natural variation dominated, and after selecting the n most informative variables based on the optimal number of variables that differentiated the pathologies from the control group. This selection process was based on the strength of association with the diseases.

Distinguishing Different Patient Phenotypes Based on Immune Markers

To estimate the effect of immune markers in discrimination across diseases, we chose to use Random Forest (RF) due to its random selection of predictors evaluated in each tree, which minimizes the impact of multicollinearity among markers, providing a broader view of potentially relevant markers. We assessed each combination of patient phenotypes using stratified 10-fold cross-validation. In each fold of the training group, we ran RF models with 5001 trees and varying maximum tree depths to regulate model generalization. The model with the best out-of-bag estimations was selected to construct the ROC curve for each fold. Finally, the 10 ROC curves were interpolated to obtain a mean curve and a 95% confidence interval. As parameter estimations were performed within each fold, there was no need for an additional evaluation group, which would be problematic given the high dimensionality and limited number of instances in the dataset. Excluding healthy individuals, we used the remaining data to train a Random Forest model with 5001 trees and a maximum tree depth limited to 8. This model was used to estimate impurity-based feature importance as described [37].

Data and code availability

Raw data for the study is available from https://data.mendeley.com/datasets/6bnzvym82c/1 (DOI: 10.17632/6bnzvym82c.1) . Source data is available as **Supplementary Spreadsheet 2**. Source code for the analysis is available on GitHub at: https://github.com/rafael-veiga/ImmunAID.git.

Acknowledgments

The authors thank all patients and volunteers enrolled in the study. This work has received funding from the European Union's Horizon 2020 research and innovation program under grant agreement No 874707 (EXIMIOUS), and No 779295 (ImmunAID). The authors acknowledge the

important contributions of Jeason Haughton and the KU Leuven FACS Core. The authors declare no conflict of interest.

References

1. Gutierrez, M.J. & Lapidus, S.K. Systemic Autoinflammatory Diseases: A Growing Family of Disorders of Overlapping Immune Dysfunction. *Rheum Dis Clin North Am* **48**, 371-395 (2022).

2. Krainer, J., Siebenhandl, S. & Weinhausel, A. Systemic autoinflammatory diseases. *J Autoimmun* **109**, 102421 (2020).

3. Ben-Chetrit, E. *et al.* Consensus proposal for taxonomy and definition of the autoinflammatory diseases (AIDs): a Delphi study. *Ann Rheum Dis* **77**, 1558-1565 (2018).

4. Tangye, S.G. *et al.* Human Inborn Errors of Immunity: 2022 Update on the Classification from the International Union of Immunological Societies Expert Committee. *J Clin Immunol* **42**, 1473-1507 (2022).

5. Zhang, J., Lee, P.Y., Aksentijevich, I. & Zhou, Q. How to Build a Fire: The Genetics of Autoinflammatory Diseases. *Annu Rev Genet* **57**, 245-274 (2023).

6. Alt, H.L. & Barker, M.H. Fever of unknown origin. *Journal of the American Medical Association* **94**, 1457-1461 (1930).

7. Ancient missense mutations in a new member of the RoRet gene family are likely to cause familial Mediterranean fever. The International FMF Consortium. *Cell* **90**, 797-807 (1997).

8. French, F.M.F.C. A candidate gene for familial Mediterranean fever. *Nat Genet* **17**, 25-31 (1997).

9. Dinarello, C.A., Wolff, S.M., Goldfinger, S.E., Dale, D.C. & Alling, D.W. Colchicine therapy for familial mediterranean fever. A double-blind trial. *N Engl J Med* **291**, 934-937 (1974).

10. Zemer, D. *et al.* A controlled trial of colchicine in preventing attacks of familial mediterranean fever. *N Engl J Med* **291**, 932-934 (1974).

11. Masters, S.L. *et al.* Familial autoinflammation with neutrophilic dermatosis reveals a regulatory mechanism of pyrin activation. *Sci Transl Med* **8**, 332ra345 (2016).

12. de Menthon, M., Lavalley, M.P., Maldini, C., Guillevin, L. & Mahr, A. HLA-B51/B5 and the risk of Behcet's disease: a systematic review and meta-analysis of case-control genetic association studies. *Arthritis Rheum* **61**, 1287-1296 (2009).

13. Gul, A. *et al.* Evidence for linkage of the HLA-B locus in Behcet's disease, obtained using the transmission disequilibrium test. *Arthritis Rheum* **44**, 239-240 (2001).

14. Remmers, E.F. *et al.* Genome-wide association study identifies variants in the MHC class I, IL10, and IL23R-IL12RB2 regions associated with Behcet's disease. *Nat Genet* **42**, 698-702 (2010).

15. Zhou, Z.Y., Chen, S.L., Shen, N. & Lu, Y. Cytokines and Behcet's disease. *Autoimmun Rev* **11**, 699-704 (2012).

16. Papa, R. *et al.* Syndrome of Undifferentiated Recurrent Fever (SURF): An Emerging Group of Autoinflammatory Recurrent Fevers. *J Clin Med* **10** (2021).

17. Watad, A. *et al.* Somatic Mutations and the Risk of Undifferentiated Autoinflammatory Disease in MDS: An Under-Recognized but Prognostically Important Complication. *Front Immunol* **12**, 610019 (2021).

18. Bleeker-Rovers, C.P. *et al.* A prospective multicenter study on fever of unknown origin: the yield of a structured diagnostic protocol. *Medicine (Baltimore)* **86**, 26-38 (2007).

19. Betrains, A., Moreel, L., De Langhe, E., Blockmans, D. & Vanderschueren, S. Rheumatic disorders among patients with fever of unknown origin: A systematic review and meta-analysis. *Semin Arthritis Rheum* **56**, 152066 (2022).

20. Mitrovic, S. & Fautrel, B. Clinical Phenotypes of Adult-Onset Still's Disease: New Insights from Pathophysiology and Literature Findings. *J Clin Med* **10** (2021).

21. Tomaras, S., Goetzke, C.C., Kallinich, T. & Feist, E. Adult-Onset Still's Disease: Clinical Aspects and Therapeutic Approach. *J Clin Med* **10** (2021).

22. Akdeniz, N., Elmas, O.F. & Karadag, A.S. Behcet syndrome: A great imitator. *Clin Dermatol* **37**, 227-239 (2019).

23. Aksentijevich, I. & Schnappauf, O. Molecular mechanisms of phenotypic variability in monogenic autoinflammatory diseases. *Nat Rev Rheumatol* **17**, 405-425 (2021).

24. Chi, H. *et al.* The landscape of innate and adaptive immune cell subsets in patients with adult-onset Still's disease. *Rheumatology (Oxford)* **63**, 1987-1997 (2024).

25. Fang, X. *et al.* B cell subsets in adult-onset Still's disease: potential candidates for disease pathogenesis and immunophenotyping. *Arthritis Res Ther* **25**, 104 (2023).

26. Myachikova, V. *et al.* Deep Immunophenotyping of Circulating T and B Cells in Relapsing Adult-Onset Still's Disease. *Curr Issues Mol Biol* **46**, 1177-1191 (2024).

27. Amariglio, N. *et al.* T-cell compartment in synovial fluid of pediatric patients with JIA correlates with disease phenotype. *J Clin Immunol* **31**, 1021-1028 (2011).

28. Mijnheer, G. & van Wijk, F. T-Cell Compartmentalization and Functional Adaptation in Autoimmune Inflammation: Lessons From Pediatric Rheumatic Diseases. *Front Immunol* **10**, 940 (2019).

29. Jung, J.Y. *et al.* Characteristic patterns of HLA presentation and T cell differentiation in adult-onset Still's disease. *Int J Immunopathol Pharmacol* **32**, 2058738418791284 (2018).

30. Huang, Z. *et al.* Type I interferon signature and cycling lymphocytes in macrophage activation syndrome. *J Clin Invest* **133** (2023).

31. Seyahi, E., Ugurlu, S., Amikishiyev, S. & Gul, A. Behcet disease, familial Mediterranean fever and MEFV variations: More than just an association. *Clin Immunol* **251**, 109630 (2023).

32. Garg, S., Wynne, K., Omoyinmi, E., Eleftheriou, D. & Brogan, P. Efficacy and safety of anakinra for undifferentiated autoinflammatory diseases in children: a retrospective case review. *Rheumatol Adv Pract* **3**, rkz004 (2019).

33. Harrison, S.R. *et al.* Anakinra as a diagnostic challenge and treatment option for systemic autoinflammatory disorders of undefined etiology. *JCI Insight* **1**, e86336 (2016).

34. Ter Haar, N.M. *et al.* Clinical characteristics and genetic analyses of 187 patients with undefined autoinflammatory diseases. *Ann Rheum Dis* **78**, 1405-1411 (2019).

35. Troyanskaya, O. *et al.* Missing value estimation methods for DNA microarrays. *Bioinformatics* **17**, 520-525 (2001).

36. Guerrero, V.M. Time-series analysis supported by power transformations. *Journal of Forecasting* **12**, 37-48 (1993).

37. Breiman, L. Random Forests. *Machine Learning*; 2001. pp. 5-31.

Tables

Table 1. Study population demographics

		Sex		Age (years)					CRP level (mg/L) †			
	N	N (%) female	P value*	Median	IQR	Min	Max	P value ^	Median	IQR	Min	Max
Healthy	58	31 (53.4%)	-	30	13.8	10	59	-	-	-	-	-
Inflammation of unknown origin	36	17 (47.2%)	0.666	44.5	32	1	76	0.425	62.5	66.1	1	342
Adult onset Still's disease (AOSD)	35	25 (71.4%)	0.118	30	12.5	16	66	0.855	91.5	106	6.3	374
Familial Mediterranean Fever (FMF)	35	23 (65.7%)	0.206	26	24	3	74	0.321	13.8	25.2	1	293
Behçet's disease	23	9 (39.1%)	0.335	23	23	6	58	0.126	20.4	26	1.4	286

IQR, interquartile range. * P value, chi-squared test of sex in relation to disease group compared to healthy. ^ P value, Mann-Whitney U test for age in relation to disease group, compared to healthy. † P value, Kruskal-Wallis test for CRP levels among disease groups = 0.736.

Figures

Figure 1. Immunological parameters associated with autoinflammation of unknown origin. Patients with autoinflammation of unknown origin (n=36) were compared against healthy individuals (n=58) by multivariate logistic regression of immunological parameters. Data from patients with Still's disease (n=35), FMF (n=35) and Behçet (n=23) are shown as reference data only. **A)** Odds ratio and 95% confidence interval of highly-associated cell population frequency changes in patients with autoinflammation of unknown origin in relation to healthy individuals. Estimated by multivariable logistic regression adjusted by sex and age. **B)** Average and 95% confidence interval of 200 times 10 fold cross-validation to evaluate a sufficient number of best cell populations, based on ability to adequately discern between autoinflammation of unknown origin and healthy individuals. **C)** Frequency for highly-associated cell populations for autoinflammation of unknown origin in relation to healthy individuals. Each dot represents a patient and each colour represents a condition. **D)** Average ROC curve with 95% confidence interval of 10 fold cross-validation for autoinflammation of unknown origin in relation to healthy individuals. ROC calculated using multi-variable logistic regression, adjusted by sex and age, considering the 40 cell populations with highest explanatory contribution. Area under ROC curve and confidence interval indicated on graph. **E)** First two PCA components of all cell populations in the dataset. Each dot represents an individual and each colour represents a condition. Histograms show distribution of values in autoinflammation of unknown origin and healthy individuals. **F)** First two PCA components of 40 cell populations most highly associated for divergence between autoinflammation of unknown origin and healthy individuals. Histograms show distribution of values in autoinflammation of unknown origin and healthy individuals. The two arrows show the direction of distinct highly associated cell populations.

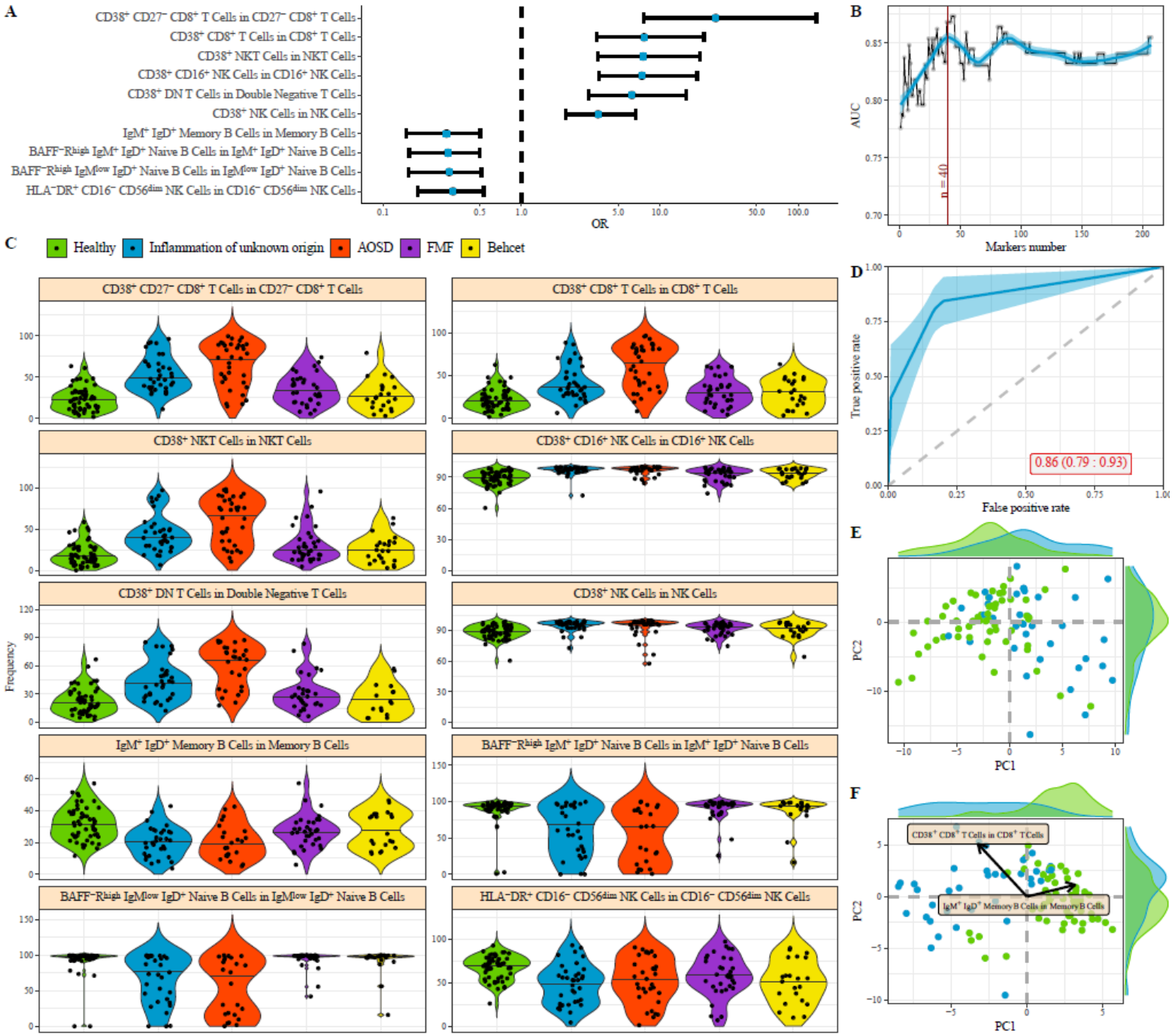
A
CD38+ CD27− CD8+ T Cells in CD27− CD8+ T Cells
CD38+ CD8+ T Cells in CD8+ T Cells
CD38+ NKT Cells in NKT Cells
CD38+ CD16+ NK Cells in CD16+ NK Cells
CD38+ DN T Cells in Double Negative T Cells
CD38+ NK Cells in NK Cells
IgM+ IgD+ Memory B Cells in Memory B Cells
BAFF−Rhigh IgM+ IgD+ Naive B Cells in IgM+ IgD+ Naive B Cells
BAFF−Rhigh IgMlow IgD+ Naive B Cells in IgMlow IgD+ Naive B Cells
HLA−DR+ CD16− CD56dim NK Cells in CD16− CD56dim NK Cells
OR
B
AUC
n = 40
Markers number
C
Healthy
Inflammation of unknown origin
AOSD
FMF
Behcet
Frequency
D
True positive rate
False positive rate
0.86 (0.79 : 0.93)
E
PC1
PC2
F
CD38+ CD8+ T Cells in CD8+ T Cells
IgM+ IgD+ Memory B Cells in Memory B Cells

Figure 2. Immunological parameters associated with AOSD. Patients with Still's disease (n=35) were compared against healthy individuals (n=58) by multivariate logistic regression of immunological parameters. Data from patients with autoinflammation of unknown origin (n=36), FMF (n=35) and Behçet (n=23) are shown as reference data only. **A)** Odds ratio and 95% confidence interval of highly-associated cell population frequency changes in patients with Still's disease in relation to healthy individuals. Estimated by multivariable logistic regression adjusted by sex and age. **B)** Average and 95% confidence interval of 200 times 10 fold cross-validation to evaluate a sufficient number of best cell populations, based on ability to adequately discern between Still's disease and healthy individuals. **C)** Frequency for highly-associated cell populations for Still's disease in relation to healthy individuals. Each dot represents a patient and each colour represents a condition. **D)** Average ROC curve with 95% confidence interval of 10 fold cross-validation for Still's disease in relation to healthy individuals. ROC calculated using multi-variable logistic regression, adjusted by sex and age, considering the 82 cell populations with highest explanatory contribution. Area under ROC curve and confidence interval indicated on graph. **E)** First two PCA components of all cell populations in the dataset. Each dot represents an individual and each colour represents a condition. Histograms show distribution of values in Still's disease and healthy individuals. **F)** First two PCA components of 82 cell populations most highly associated for divergence between Still's disease and healthy individuals. Histograms show distribution of values in Still's disease and healthy individuals. The two arrows show the direction of distinct highly associated cell populations.

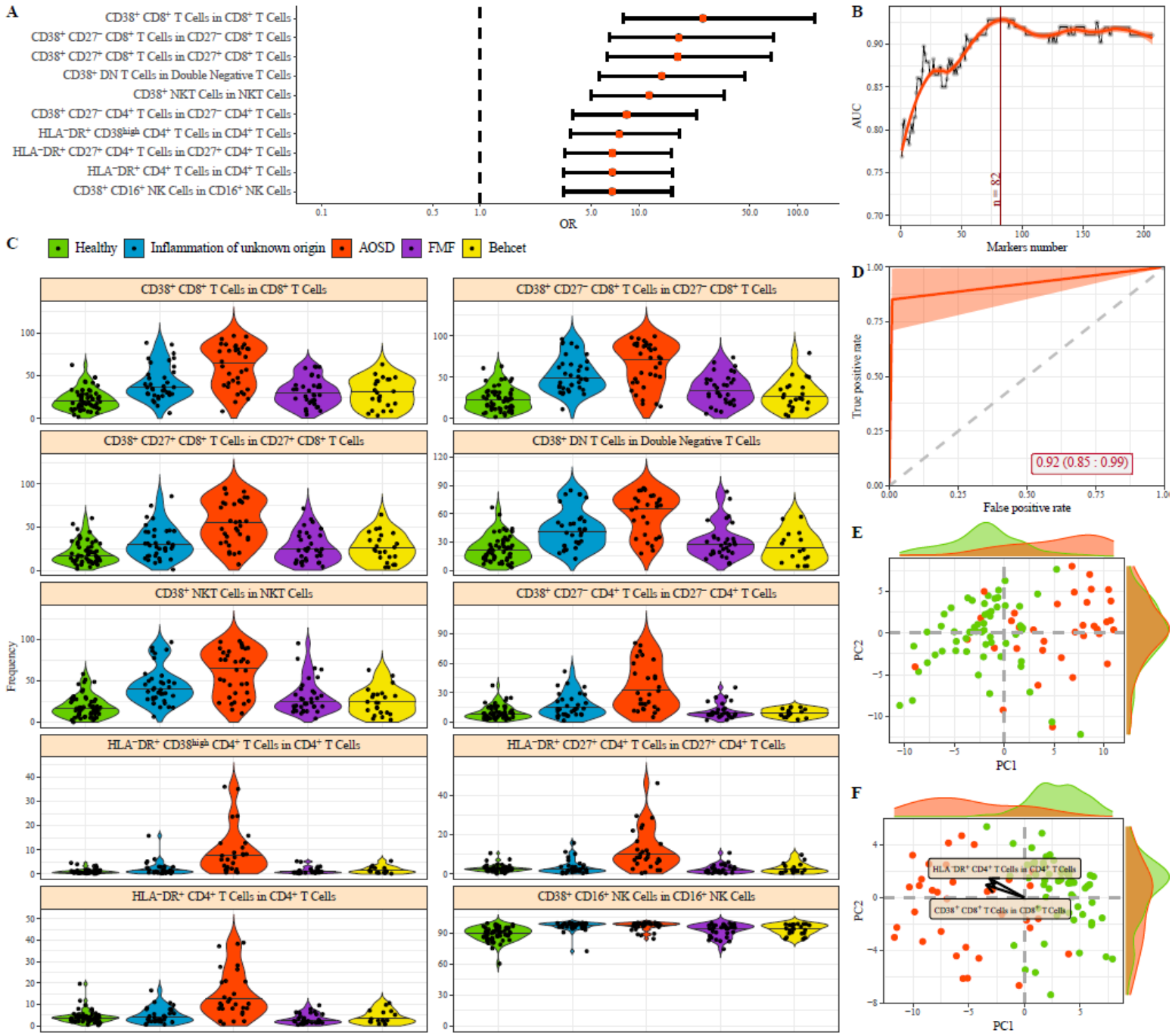
A
CD38+ CD8+ T Cells in CD8+ T Cells
CD38+ CD27− CD8+ T Cells in CD27− CD8+ T Cells
CD38+ CD27+ CD8+ T Cells in CD27+ CD8+ T Cells
CD38+ DN T Cells in Double Negative T Cells
CD38+ NKT Cells in NKT Cells
CD38+ CD27− CD4+ T Cells in CD27− CD4+ T Cells
HLA−DR+ CD38high CD4+ T Cells in CD4+ T Cells
HLA−DR+ CD27+ CD4+ T Cells in CD27+ CD4+ T Cells
HLA−DR+ CD4+ T Cells in CD4+ T Cells
CD38+ CD16+ NK Cells in CD16+ NK Cells
OR
B
AUC
Markers number
n = 82
C
Healthy
Inflammation of unknown origin
AOSD
FMF
Behcet
Frequency
D
True positive rate
False positive rate
0.92 (0.85 : 0.99)
E
PC1
PC2
F
PC1
PC2

Figure 3. Immunological parameters associated with FMF. Patients with FMF (n=35) were compared against healthy individuals (n=58) by multivariate logistic regression of immunological parameters. Data from patients with autoinflammation of unknown origin (n=36), Still's disease (n=35) and Behçet (n=23) are shown as reference data only. **A)** Odds ratio and 95% confidence interval of highly-associated cell population frequency changes in patients with FMF in relation to healthy individuals. Estimated by multivariable logistic regression adjusted by sex and age. **B)** Average and 95% confidence interval of 200 times 10 fold cross-validation to evaluate a sufficient number of best cell populations, based on ability to adequately discern between FMF and healthy individuals. **C)** Frequency for highly-associated cell populations for FMF in relation to healthy individuals. Each dot represents a patient and each colour represents a condition. **D)** Average ROC curve with 95% confidence interval of 10 fold cross-validation for FMF in relation to healthy individuals. ROC calculated using multi-variable logistic regression, adjusted by sex and age, considering the 55 cell populations with highest explanatory contribution. Area under ROC curve and confidence interval indicated on graph. **E)** First two PCA components of all cell populations in the dataset. Each dot represents an individual and each colour represents a condition. Histograms show distribution of values in FMF and healthy individuals. **F)** First two PCA components of **55** cell populations most highly associated for divergence between FMF and healthy individuals. Histograms show distribution of values in FMF and healthy individuals. The two arrows show the direction of distinct highly associated cell populations.

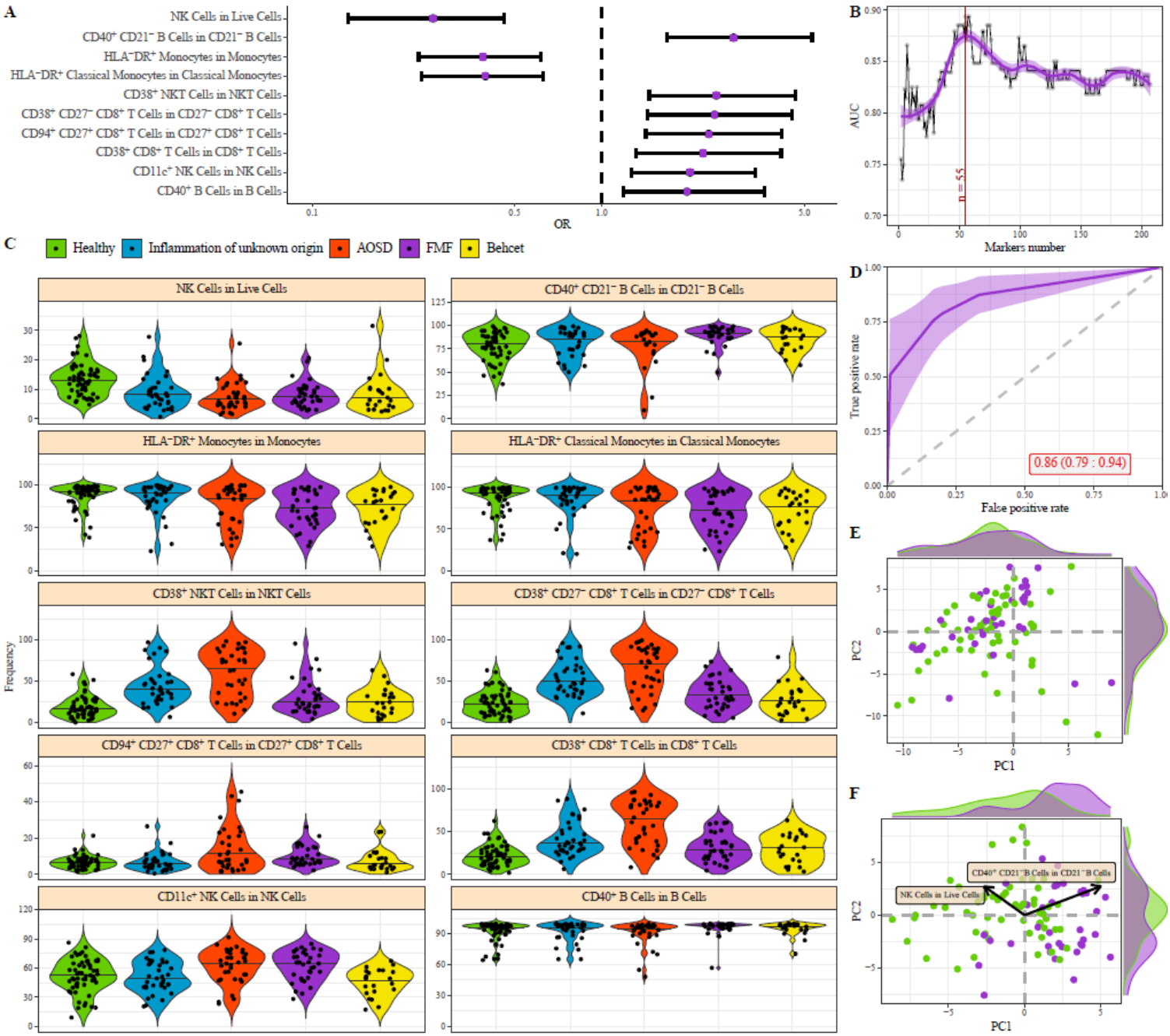
A
NK Cells in Live Cells
CD40+ CD21− B Cells in CD21− B Cells
HLA−DR+ Monocytes in Monocytes
HLA−DR+ Classical Monocytes in Classical Monocytes
CD38+ NKT Cells in NKT Cells
CD38+ CD27− CD8+ T Cells in CD27− CD8+ T Cells
CD94+ CD27+ CD8+ T Cells in CD27+ CD8+ T Cells
CD38+ CD8+ T Cells in CD8+ T Cells
CD11c+ NK Cells in NK Cells
CD40+ B Cells in B Cells
OR
B
AUC
Markers number
n = 55
C
Healthy
Inflammation of unknown origin
AOSD
FMF
Behcet
Frequency
D
True positive rate
False positive rate
0.86 (0.79 : 0.94)
E
PC1
PC2
F
CD40+ CD21−B Cells in CD21−B Cells
NK Cells in Live Cells

Figure 4. Immunological parameters associated with Behçet's disease. Patients with Behçet's disease (n=23) were compared against healthy individuals (n=58) by multivariate logistic regression of immunological parameters. Data from patients with autoinflammation of unknown origin (n=36), Still's disease (n=35) and FMF (n=35) are shown as reference data only. **A)** Odds ratio and 95% confidence interval of highly-associated cell population frequency changes in patients with Behçet in relation to healthy individuals. Estimated by multivariable logistic regression adjusted by sex and age. **B)** Average and 95% confidence interval of 200 times 10 fold cross-validation to evaluate a sufficient number of best cell populations, based on ability to adequately discern between Behçet and healthy individuals. **C)** Frequency for highly-associated cell populations for Behçet in relation to healthy individuals. Each dot represents a patient and each colour represents a condition. **D)** Average ROC curve with 95% confidence interval of 10 fold cross-validation for Behçet in relation to healthy individuals. ROC calculated using multi-variable logistic regression, adjusted by sex and age, considering the 61 cell populations with highest explanatory contribution. Area under ROC curve and confidence interval indicated on graph. **E)** First two PCA components of all cell populations in the dataset. Each dot represents an individual and each colour represents a condition. Histograms show distribution of values in Behçet and healthy individuals. **F)** First two PCA components of 61 cell populations most highly associated for divergence between Behçet and healthy individuals. Histograms show distribution of values in Behçet and healthy individuals. The two arrows show the direction of distinct highly associated cell populations.

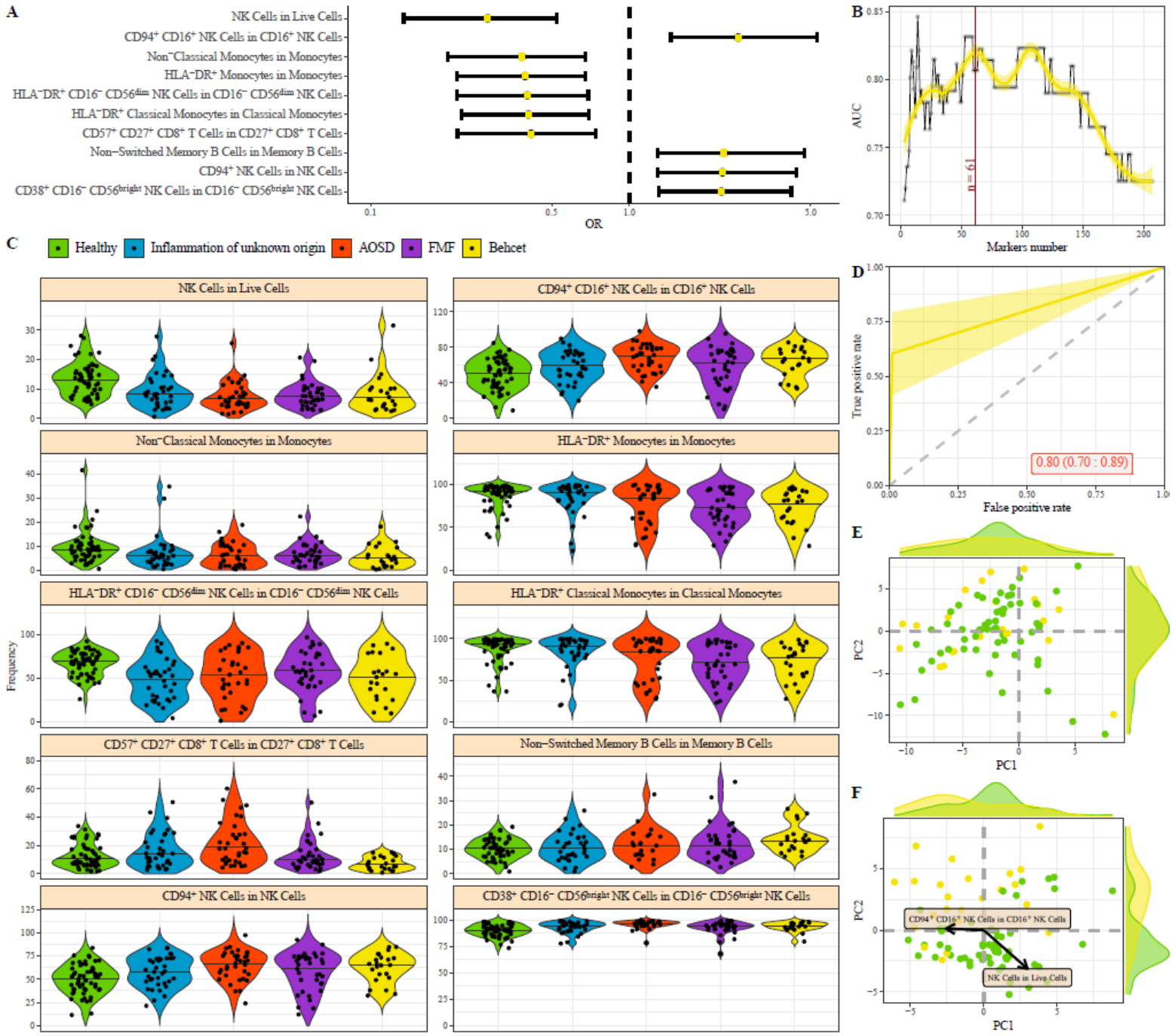
A
NK Cells in Live Cells
CD94+ CD16+ NK Cells in CD16+ NK Cells
Non−Classical Monocytes in Monocytes
HLA−DR+ Monocytes in Monocytes
HLA−DR+ CD16− CD56dim NK Cells in CD16− CD56dim NK Cells
HLA−DR+ Classical Monocytes in Classical Monocytes
CD57+ CD27+ CD8+ T Cells in CD27+ CD8+ T Cells
Non−Switched Memory B Cells in Memory B Cells
CD94+ NK Cells in NK Cells
CD38+ CD16− CD56bright NK Cells in CD16− CD56bright NK Cells
OR
B
AUC
Markers number
n = 61
C
Healthy
Inflammation of unknown origin
AOSD
FMF
Behcet
Frequency
D
True positive rate
False positive rate
0.80 (0.70 : 0.89)
E
PC1
PC2
F
CD94+ CD16+ NK Cells in CD16+ NK Cells
NK Cells in Live Cells

Figure 5. Machine learning-led multi-disease comparison clusters autoinflammation of unknown origin patients with Still's disease patients. A multi-disease comparison was performed using immune phenotypes from patients with autoinflammation of unknown origin (n=36), Still's disease (n=35), FMF (n=35) and Behçet (n=23). Healthy individuals are shown as reference data only, not being used to build immuno-discriminating models. In the upper-right panels, a Random Forest algorithm was built to discriminate between diseases, with the Receiver Operating Characteristic (ROC) curve shown for each pairwise comparison of disease-disease and healthy-disease. The black line represents the average ROC curve obtained from 10-fold cross-validation. The shaded gray area indicates the 95% confidence interval. The numeric labels within the plots show the average area under the ROC curve (AUC) and the 95% confidence interval for each comparison. In the lower-left panels, individuals are plotted on the first two principal components for the respective comparison.

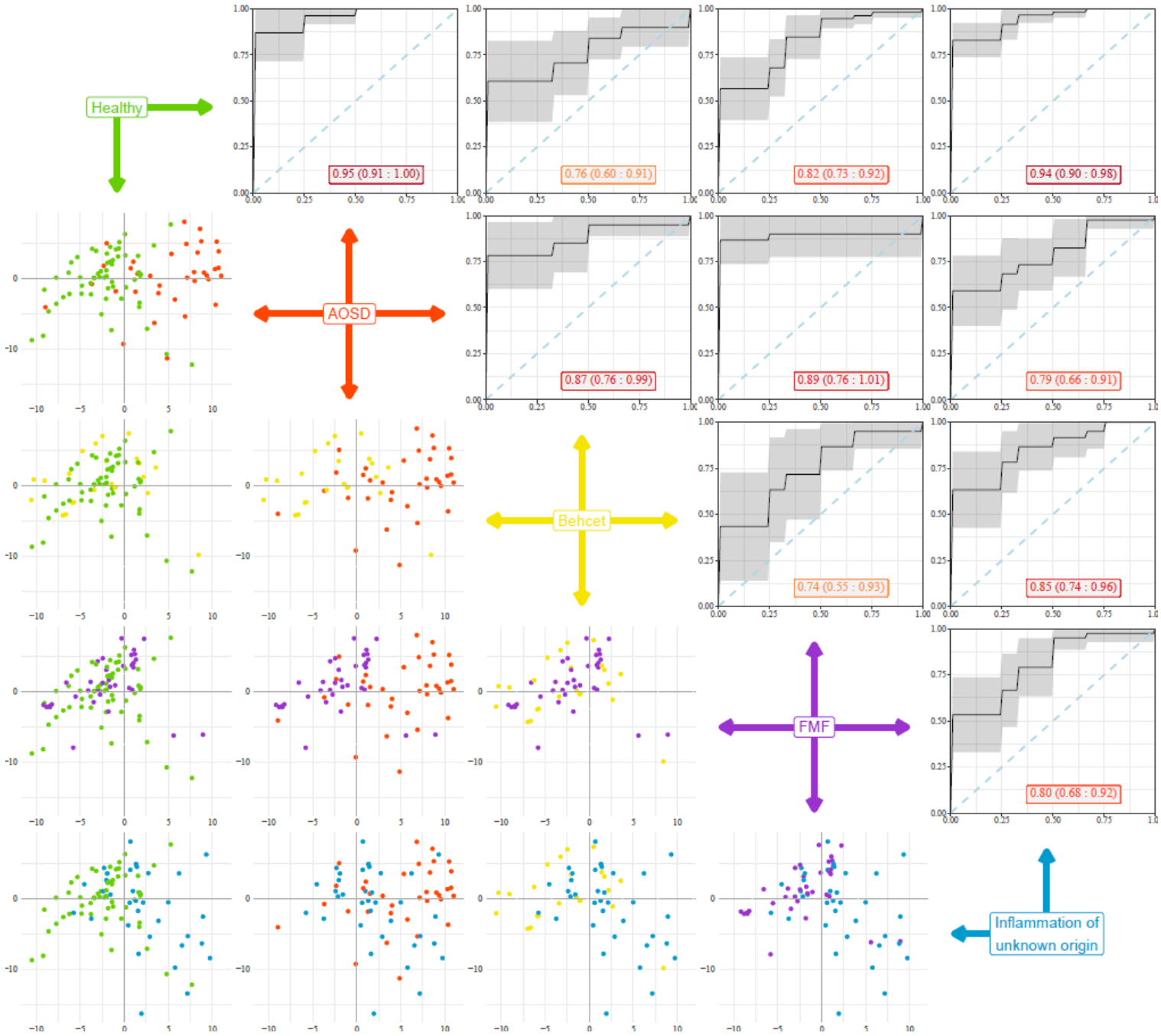
Healthy
0.95 (0.91 : 1.00)
0.76 (0.60 : 0.91)
0.82 (0.73 : 0.92)
0.94 (0.90 : 0.98)
AOSD
0.87 (0.76 : 0.99)
0.89 (0.76 : 1.01)
0.79 (0.66 : 0.91)
Behcet
0.74 (0.55 : 0.93)
0.85 (0.74 : 0.96)
FMF
0.80 (0.68 : 0.92)
Inflammation of unknown origin

Figure 6. Key immunological features driving machine learning-led disease identification. A multi-disease comparison was performed using a Random Forest algorithm to identify immune characteristics with discriminating potential between patients with autoinflammation of unknown origin (n=36), AOSD (n=35), FMF (n=35) and Behçet (n=23). Healthy individuals were not used in the model generation, and are shown as reference data only. Frequency for the 16 highest associated cell populations for disease discrimination. Each dot represents a patient and each colour represents a condition.

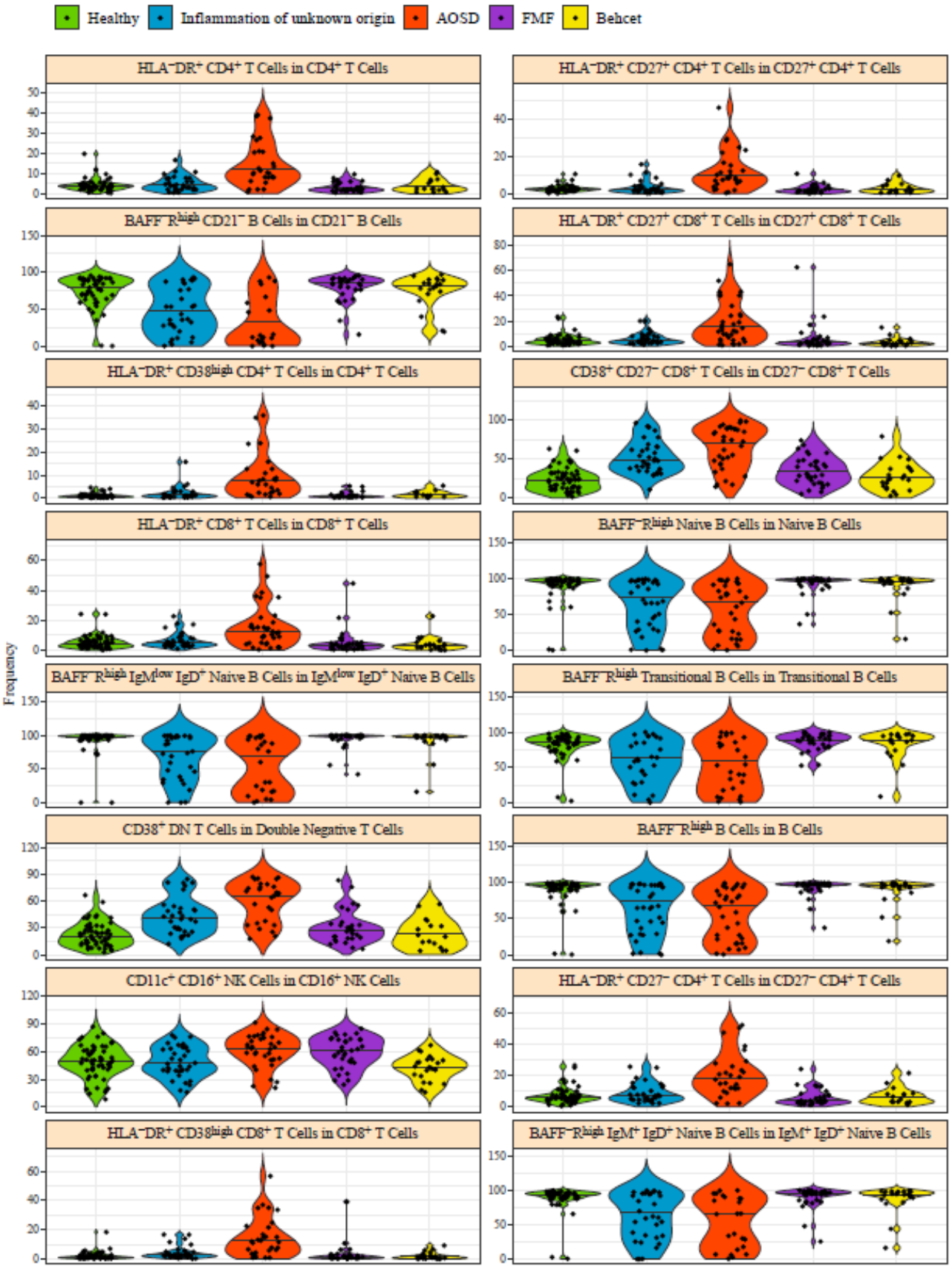
Healthy
Inflammation of unknown origin
AOSD
FMF
Behcet
HLA⁻DR⁺ CD4⁺ T Cells in CD4⁺ T Cells
HLA⁻DR⁺ CD27⁺ CD4⁺ T Cells in CD27⁺ CD4⁺ T Cells
BAFF⁻R^high CD21⁻ B Cells in CD21⁻ B Cells
HLA⁻DR⁺ CD27⁺ CD8⁺ T Cells in CD27⁺ CD8⁺ T Cells
HLA⁻DR⁺ CD38^high CD4⁺ T Cells in CD4⁺ T Cells
CD38⁺ CD27⁻ CD8⁺ T Cells in CD27⁻ CD8⁺ T Cells
HLA⁻DR⁺ CD8⁺ T Cells in CD8⁺ T Cells
BAFF⁻R^high Naive B Cells in Naive B Cells
BAFF⁻R^high IgM^low IgD⁺ Naive B Cells in IgM^low IgD⁺ Naive B Cells
BAFF⁻R^high Transitional B Cells in Transitional B Cells
CD38⁺ DN T Cells in Double Negative T Cells
BAFF⁻R^high B Cells in B Cells
CD11c⁺ CD16⁺ NK Cells in CD16⁺ NK Cells
HLA⁻DR⁺ CD27⁻ CD4⁺ T Cells in CD27⁻ CD4⁺ T Cells
HLA⁻DR⁺ CD38^high CD8⁺ T Cells in CD8⁺ T Cells
BAFF⁻R^high IgM⁺ IgD⁺ Naive B Cells in IgM⁺ IgD⁺ Naive B Cells
Frequency